18th Australasian Fluid Mechanics Conference
Launceston, Australia
3-7 December 2012

A Numerical Investigation of Supersonic Cavity Flow At Mach 2

V. Sridhar, S. L. Gai and H. Kleine

School of Engineering & IT
The University of New South Wales, Canberra, Canberra 2600, Australia

Abstract

Numerical simulations were carried out for a two-dimensional shallow cavity with a length-to-depth ratio of 8 in a Mach 2 flow. The simulations were carried out with an in-house code (Eilmer-3) and then compared with the results obtained with the commercially available package FLUENT and experimental data. The standard Wilcox $k-\omega$ turbulence model was used to model turbulence in the simulations. While the numerically predicted frequencies generally match experimental data, the dominant frequency does not. Similarly, a difference in pressure level and amplitude between simulation and experiment is observed. Both codes which differ substantially in their structure, predict the flow phenomena in a near identical way, which gives confidence in the validity of the results obtained.

Introduction

The study of compressible cavity flow is an important research topic in the field of aerodynamics and acoustics. Although the geometry of these cavities is simple, their unsteady fluid dynamic behaviour is complicated and difficult to predict both in subsonic and supersonic flows. These fluid phenomena typically cause unwanted drag, structural noise and vibrations. Cavities are classified based on the length-to-depth ratio (L/D), where L is the length of the cavity and D is the depth. Cavities are called 'open' if $L/D < 10$, 'closed' if $L/D > 13$ and 'transitional' for $10 \leq L/D \leq 13$. In case of open cavities, the boundary layer separates from the leading edge and forms a shear layer which bridges the length of the cavity. This shear layer impinges on the rear wall of the cavity, and a pressure wave is created which will travel upstream inside the cavity, interact with the shear layer and thereby cause a feedback loop. This feedback mechanism produces discrete resonant frequencies [5] [8] [11]. The present study investigates numerically the open cavity resonance and variation of the associated flow field by using two different numerical codes, the in-house Eilmer-3 and the commercial package FLUENT, for a cavity with L/D of 8 in a Mach 2 free stream.

Geometry and Flow conditions

The cavity investigated here has a geometry as shown in Fig. 1. It comprises of an upstream flat-plate of length $l = 184\,\text{mm}$, followed by a cavity with a depth $D = 4\,\text{mm}$ and length-to-depth ratio $L/D = 8$, and another flat plate. The experimental work on this configuration was conducted in a supersonic wind tunnel at Mach 2 and Reynolds number $Re_l = 4.6 \times 10^6$. The tunnel test time was approximately 30 s and time-resolved measurements were made during a 4 s window within this period. In the numerical simulations a flow time of 6 ms was used which corresponds to a characteristic time $tU_\infty/D = 763$. This was chosen after doing some initial tests to evaluate the times required for flow establishment over the upstream flat plate and also for reaching steady amplitude periodic oscillations in the cavity. It was found that the flow field of interest was fully established after approximately ≈1 ms and that an overall flow time of 6 ms was fully adequate to analyse the flow behaviour. The initial calculations showed that extending the calculations to larger times did not change the results but only increased the computational effort. The free stream conditions are based on the experimental data and are given in Table 1.

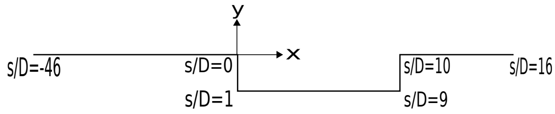

Figure 1: Cavity geometry

Table 1: Free stream conditions

M_∞	P_∞	T_∞	Re_l	k_∞	ω_∞
–	Pa	K	–	m^2/s^2	1/s
2	25560.9	161	4.6x10^6	3886	1.9x10^6

Numerical Details

Grid Independence

In the present work numerical simulation of a two-dimensional flow over a cavity is carried out using two CFD codes, the in-house code Eilmer-3 and the commercial CFD package FLUENT. Eilmer-3 is a code developed by Jacobs et al. [4] at the University of Queensland for simulating time accurate compressible flow in two and three dimensions. It is based on a finite-volume formulation of mass, momentum, energy and species conservation equations and is implemented on block-structured grids. It has capabilities of solving both laminar and turbulent flows. It has a standard Wilcox $k-\omega$ turbulence model [10] to compute the turbulence parameters k and ω (Eqns. 1 and 2). The MUSCL scheme is used to obtain second order accuracy in spatial dimensions. The AUSMDV [9] scheme is used to calculate the fluxes. In the present instance, the code is used to predict the behaviour of a turbulent compressible flow in and around a cavity. The viscosity of the fluid (air) is modeled using Sutherland's formulation. Free stream turbulence parameters are calculated based on equations 1 and 2. The co-ordinate system is non-dimensionalised based on the cavity depth (D), and the wetted distance s, thus $s/D = 0$ is the top corner of cavity front face and $s/D = 1$ is the bottom corner of cavity front face. $s/D = 9$ is the bottom corner of rear face and $s/D = 10$ is the top corner of the cavity rear face (Fig. 1). The commercially available grid generation software ICEM-CFD was used to create multi-block structured grids. The grid is shown in Fig. 2.

$$k = \frac{3}{2}(I_{turb}U_\infty)^2 \tag{1}$$

where I_{turb} is the turbulent intensity.

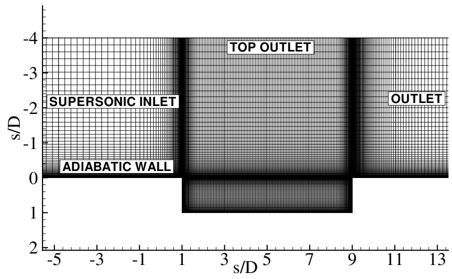

Figure 2: Computational domain of the cavity

$$\omega = \rho_\infty \frac{k}{\mu_{lam}} \left(\frac{\mu_{lam}}{\mu_{turb}} \right) \tag{2}$$

where μ_{lam} and μ_{turb} are the laminar and turbulent viscosities and ρ_∞ is the density of the free stream.

The inlet condition is a supersonic inflow, the wall is adiabatic and the top and outer edge are given as pressure outlets. The grid is clustered at the walls and expanded in $y-$direction with an expansion ratio of 1.1 using the hyperbolic law. The grids at the inlet and near to the cavity are also expanded with an expansion ratio of 1.1 using the bi-geometric law. For the cells near the cavity leading edge upper corner and trailing edge upper corner it was ensured that $\Delta x = \Delta y = \Delta_w$. Such clustering of grids is needed to capture the boundary layer and separation regions where the gradients are high and also to accurately calculate skin friction. A grid independence study was carried out with five different grids (see table 2). The grid size was doubled in both x and y directions for the first three grids and the first cell height were 50 µm, 25 µm and 10 µm respectively. It has been shown by Mohri and Hillier [5] that skin friction and heat flux are generally very sensitive to grid size. As the wall here is adiabatic, the skin friction coefficient C_f and the non-dimensionalised pressure $\mathrm{p}/\mathrm{p}_\infty$ have been used as the variables for the grid independence study. The CFL (Courant-Friedrichs-Lewy condition) given by equation 3 number was 0.5. The time step was $\approx 4 \times 10^{-10}$s.

$$\mathrm{CFL} = \frac{\mathrm{u}\Delta \mathrm{t}}{\Delta \mathrm{x}} \tag{3}$$

where u is the local velocity, Δx is the grid spacing and Δt is the time step.

Table 2: Different grids used for the grid independence study

Grid	Upstream	Cavity	Downstream	Δ_w
G1	40×15	27×10	15×15	50 µm
G2	80×30	54×20	30×30	25 µm
G3	160×60	108×40	60×60	10 µm
G4	240×60	162×60	90×60	10 µm
G5	240×90	266×80	90×90	10 µm

The grid independence study of highly unsteady oscillating flows is difficult [5]. Time-averaged C_f and p/p_∞ are therefore used to check for convergence. It can be seen in Figs. 3 and 4 that the first two grid calculations are inaccurate and the boundary layer is not well captured. This can be due to $y+ > 1$ in the first cell and also insufficient cells in the boundary layer. It can be seen from G3 to G5 that there is no variation of C_f or p/p_∞ over the flat plate as $\Delta_w = 10\mu m$ was constant and also $y+ < 1$ and $y+ = u+$ in the first cell which ensured that the first cell is within the viscous sub-layer. Since the boundary layer flow is a steady state solution, the variables C_f and p/p_∞ match for G3 to G5. In the cavity the skin friction seems to have converged for G4 to G5. This is in variance with Mohri and Hillier [5] where they found that the skin friction did not converge in the cavity even after time averaging. Due to highly increased computation times, computations with $\Delta_w < 10\mu m$ were not pursued. For all further computations grid G4 was used as it was possible to capture all the flow physics and frequencies when compared with experiments.

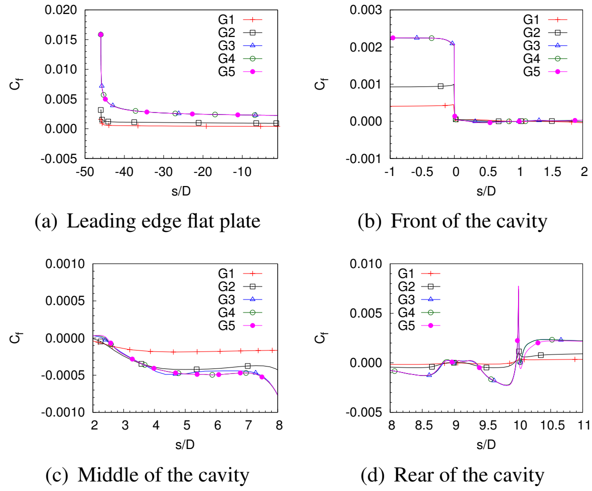

(a) Leading edge flat plate (b) Front of the cavity

(c) Middle of the cavity (d) Rear of the cavity

Figure 3: Skin friction distribution with different grids

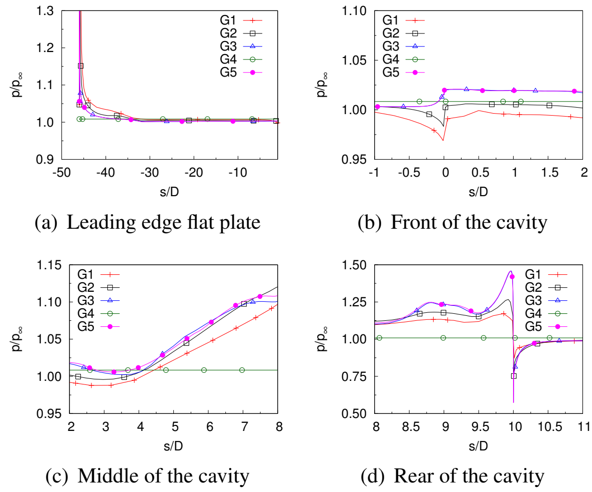

(a) Leading edge flat plate (b) Front of the cavity

(c) Middle of the cavity (d) Rear of the cavity

Figure 4: Normalised pressure distribution with different grids

Methodology

Grid G4 was also used in FLUENT to simulate the supersonic flow over the cavity. Explicit time stepping was applied to achieve time-accurate simulations. The density-based solver was used as it is better suited for compressible flows [1]. The Roe flux [7] scheme was incorporated to calculate fluxes and a second order scheme was used for accuracy. FLUENT was used here alongside with Eilmer-3 basically to verify the Eilmer-3 code. The Eilmer-3 code was originally developed for hypersonic flows and its use here for a supersonic unsteady flow is new. Roache [6] and Harvey et al. [2] point out that comparing the solutions from two different codes can be a method of code verification.

The flow was assumed to be fully turbulent from the leading edge of the flat plate. The velocity inside the cavity was initialised to zero and the domain above the cavity was initialised with the free stream conditions shown in table 1. The thickness of the boundary layer approaching the cavity leading edge was 2.7mm in the simulations, which is in good agreement with the experimentally measured boundary layer thickness of 2.8 ± 0.2mm.

Results & Discussion

Pressure and Frequency Spectra

Figures 5(a) to 5(f) show numerical and experimental pressure time history and frequency spectra obtained at location 0.625L on the cavity floor.

Considering pressure first, it is seen that with Eilmer-3, the flow attains a steady oscillatory state after a characteristic time of about 150. In FLUENT simulations, this time is $\approx$200 (Fig. 5(a) and 5(c)). The steady state amplitude in both cases is small. The experimental results, Fig. 5(e), show that the mean steady state pressure level is lower by about 15% when compared with the simulation results, but the amplitudes are considerably higher ($\approx$ 50%). The latter difference between experiment and simulation is caused by the noise present in the transducer and measurement system.

Figures 5(b), 5(d) and 5(f) show the frequency spectra from computations as well as experiments. Seven resonant peaks can be identified in the range from 3kHz to 40kHz. The sound pressure level (SPL) predictions, however, vary considerably between the simulations and the experimental data. The two simulations predict nearly identical SPL at corresponding frequencies but the SPL results from the experiment are consistently higher by 5dB to 10dB.

From the frequency spectra, we also note that while the experimental data show a clearly dominant frequency at mode 1, the simulations show mode 1 to be dominant in Eilmer-3 and mode 3 in FLUENT. Figure 6 shows a comparison of Strouhal numbers from the two simulations, experimental data, as well as from the modified Rossiter formula [3].The two simulations show reasonably good agreement with each other, with the experiments as well as the Rossiter formula, in particular for modes 2 and 3. For higher modes ($m \geq 4$), the Eilmer-3 code seems to overpredict frequencies by 4 to 9 percent in comparison with experiment. The small differences in frequencies between the two codes are possibly due to different flux schemes.

Cavity Flow Features

The contour plots of normalised density, Mach number and streamline patterns around the cavity are shown in Fig. 8(a), 8(b) and 8(c). From the normalised density contours we note that both Eilmer-3 and FLUENT capture the flow phenomena well when compared with experimental visualisations (Fig. 7). It is seen from the contour plots that a thick shear layer is formed bridging the cavity length. A shock at the leading edge top corner of the cavity is formed as a consequence of the lifting of the shear layer. There is an impingement shock established at the trailing edge followed by an expansion and again a weak compression shock generated due to reattachment of the shear layer on the flat plate after the cavity. The recirculation region inside the cavity is evident. There are some differences between the two computations, especially in the shear layer and inside the cavity. The lifting effect of the shear layer at the leading edge and impingement at the trailing edge seems to be more pronounced with Eilmer-3 compared with that of FLUENT.

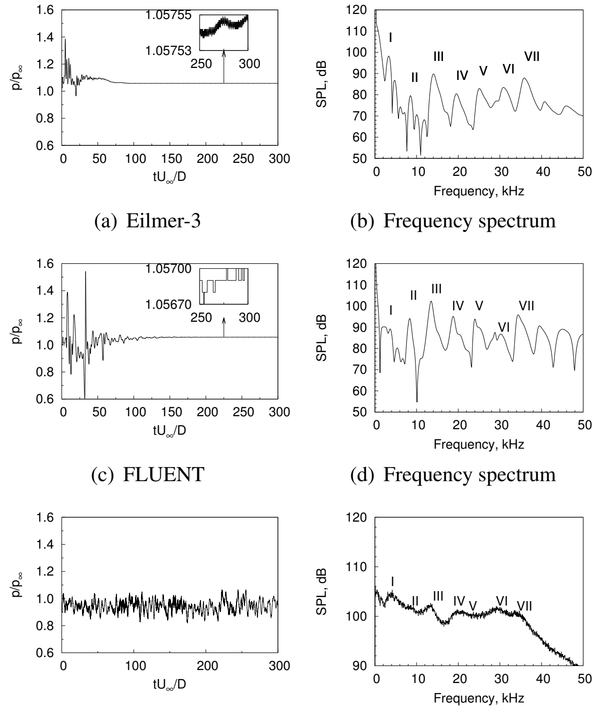

(a) Eilmer-3 (b) Frequency spectrum

(c) FLUENT (d) Frequency spectrum

(e) Experiment (f) Frequency spectrum

Figure 5: Normalised pressure time plot and frequency spectra for Eilmer-3, FLUENT and experiment at location 0.625L

The Mach number contours in Fig. 8(b) are very similar with small differences in the trailing edge impingement region. The streamline patterns (Fig. 8(c)) are almost identical. Both show the presence of two main vortices, one close to the leading edge and the other covering the length of the cavity. There are also two small secondary vortices near the leading and trailing edge bottom corners. FLUENT predicts a larger vortex near the leading edge than Eilmer-3, but the overall features are similar in both simulations. The dividing streamline plots of Eilmer-3 and FLUENT (Fig. 8(d)) clearly show that the streamline impinges just below the trailing edge top corner and then establishes itself at the trailing edge rear plate. This shear layer impinge-

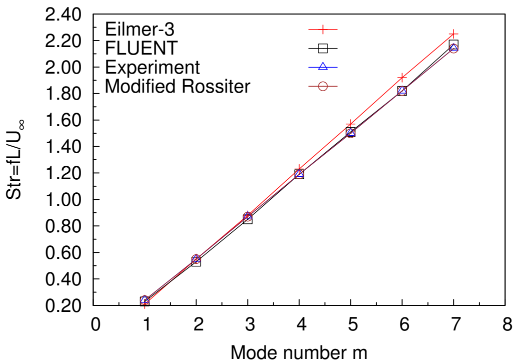

Figure 6: Comparison of Strouhal numbers

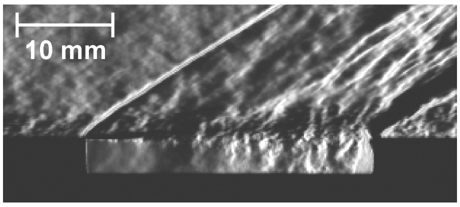

Figure 7: Instantaneous schlieren visualisation(exposure time = 1μs)

ment causes the shear layer to slightly lift thereby causing an impingement shock preceded by an expansion fan. The dividing streamline velocity from both computations was $0.36U_\infty$.

Conclusions

Numerical simulations of turbulent compressible flow over a rectangular shallow cavity of length to depth ratio 8 in a Mach 2 free stream using two different codes, Eilmer-3 (an in-house code) and the commercial code FLUENT are presented. The results are compared with experimental data.

The results from the two codes agreed reasonably well with each other and also with experiments although Eilmer-3 slightly overpredicts frequencies above mode 3 when compared with Rossiter, FLUENT and experiments. For the predictions presented, however, neither FLUENT nor Eilmer-3 provides reasonable estimates of the magnitudes of each mode and both codes also predict a different dominant mode when compared to experimental results.

Detailed features of flow over and within the cavity are highlighted emphasising the finer details near the cavity leading and trailing edges. Both codes yield very similar results with some minor differences between them which cannot be clarified by comparison with experimental records as the actual flow in the cavity is 3D, so that our regular line-of-sight visualization techniques cannot resolve such fine features.

The results have shown that the Eilmer-3 code, originally developed for hypersonic reacting and non-reacting flows, yields reasonable data for supersonic unsteady separating and reattaching flows.

Acknowledgements

The authors would like to express their sincere thanks to Dr. Peter Jacobs of the University of Queensland for allowing us to use his Eilmer-3 code and also for his help in its application.

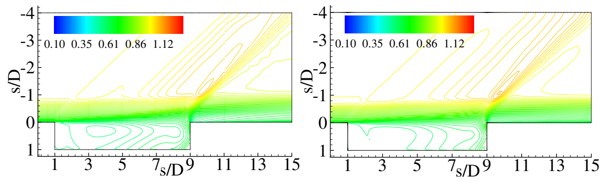

(a) Normalised density ρ/ρ_∞ contours

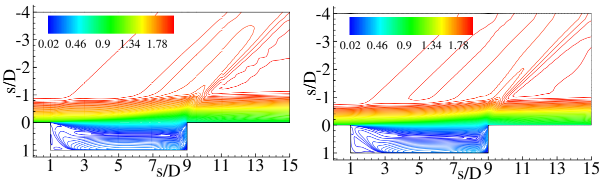

(b) Mach contours

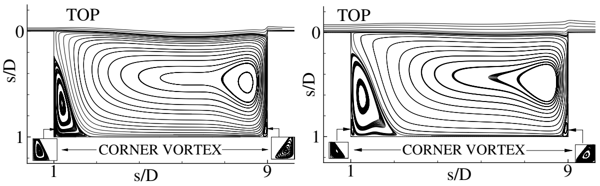

(c) Streamlines

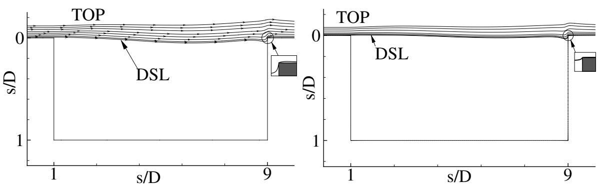

(d) Dividing streamline (DSL)

Figure 8: Cavity flow features at 3 ms ($tU_\infty/D = 381$)

References

[1] *ANSYS 13 Documentation*, 2010.

[2] Harvey, J., Holden, M. and Wadhams, T., Code validation study of laminar shock boundary layer and shock/shock interactions in hypersonic flow part b: Comparison with Navier-Stokes and DSMC solutions, in *39th Aerospace Sciences Meeting and Exhibit, Jan 8-11*, Reno, Nevada, 2001, number 1031.

[3] Heller, H. H. and Bliss, D. B., Aerodynamically induced resonance in rectangular cavities: Physical mechanisms and supression concepts, Technical Report AFFDL-TR-74-133, Wright-Patterson Air Force Base, 1975.

[4] Jacobs, P., Gollan, R., Denman, A., O'Flaherty, B., Potter, D., Petrie-Repar, P. and Johnston, I., Eilmer's theory book: Basic models for gas dynamics and thermochemistry, Technical report, University of Queensland, Brisbane, 2010.

[5] Mohri, K. and Hillier, R., Computational and experimental study of supersonic flow over axisymmetric cavities, *Shock Waves*, **21**, 2011, 175–191.

[6] Roache, P., Quantification of uncertainty in computational fluid dynamics, *Annual Review of Fluid Mechanics*, **29**, 1997, 123–160.

[7] Roe, P., Approximate Riemann Solvers, Parameter Vectors, and Difference Schemes, *Journal of Computational Physics*, **43**, 1981, 357–373.

[8] Rossiter, J., Wind tunnel experiments on the flow over rectangular cavities at subsonic and transonic speeds, Technical Report 3438, Aeronautical Research Council, 1964.

[9] Wada, Y. and Liou, M., A flux splitting scheme with high-resolution and robustness for discontinuities, in *32nd Aerospace Sciences Meeting and Exhibit, Jan 10-13*, Reno, Nevada, 1994, number 0083.

[10] Wilcox, D. C., Turbulence modelling for CFD, Technical Report 3, DCW Industries, California,USA, 2006.

[11] Zhang, X. and Edwards, J., An investigation of supersonic oscillatory cavity flows driven by thick shear layers, *Aeronautical Journal*, **94**, 1990, 355–364.